

Efficient Architecture Search for Diverse Tasks

Junhong Shen^{* 1} Mikhail Khodak^{* 1} Ameet Talwalkar¹

Abstract

While neural architecture search (NAS) has enabled automated machine learning (AutoML) for well-researched areas, its application to tasks beyond computer vision is still under-explored. As less-studied domains are precisely those where we expect AutoML to have the greatest impact, in this work we study NAS for efficiently solving *diverse* problems. Seeking an approach that is fast, simple, and broadly applicable, we fix a standard convolutional network (CNN) topology and propose to search for the right kernel sizes and dilations its operations should take on. This dramatically expands the model’s capacity to extract features at multiple resolutions for different types of data while only requiring search over the operation space. To overcome the efficiency challenges of naive weight-sharing in this search space, we introduce DASH, a differentiable NAS algorithm that computes the mixture-of-operations using the Fourier diagonalization of convolution, achieving both a better asymptotic complexity and an up-to-10x search time speedup in practice. We evaluate DASH on NAS-Bench-360, a suite of ten tasks designed for benchmarking NAS in diverse domains. DASH outperforms state-of-the-art methods in aggregate, attaining the best-known automated performance on seven tasks. Meanwhile, on six of the ten tasks, the combined search and retraining time is less than 2x slower than simply training a CNN backbone that is far less accurate.

1. Introduction

The success of deep learning for computer vision and natural language processing has spurred growing interest in enabling similar breakthroughs for other domains such as biology, healthcare, and physical sciences. Consequently, there is enormous potential for neural architecture search to help automate model development for diverse tasks. How-

Preprint. Under review. ^{*}Equal contribution ¹Carnegie Mellon University. Correspondence to: Junhong Shen <junhongs@andrew.cmu.edu>, Mikhail Khodak <khodak@cmu.edu>, Ameet Talwalkar <talwalkar@cmu.edu>.

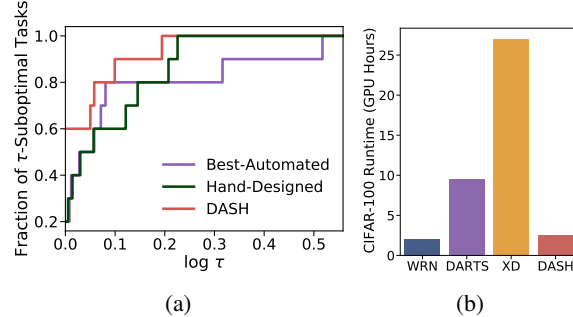


Figure 1: (a) Comparing the aggregate performance of the best AutoML methods (task-wise), hand-designed models, and DASH on NAS-Bench-360 via performance profiles (defined in Section 4.2). Larger values are better, as they represent a larger fraction of tasks on which the method is within a multiplicative factor τ of the best. (b) Runtime for Wide ResNet, DARTS, XD, and DASH on CIFAR-100. XD is too expensive to be applied to many other NAS-Bench-360 tasks (Roberts et al., 2021; Tu et al., 2021).

ever, while extensive NAS research has been devoted to improving the search speed (Pham et al., 2018; Liu et al., 2019b) and automatically attaining state-of-the-art performance on CIFAR and ImageNet (Li et al., 2021a), the resulting algorithms have subpar performance beyond the datasets on which they were developed. For example, in the analysis of NAS-Bench-360 (Tu et al., 2021), a recent benchmark designed for improving task diversity in NAS evaluation, the authors show a significant gap between models found by NAS methods, such as DARTS (Liu et al., 2019b) and DenseNAS (Fang et al., 2020), and hand-crafted architectures on a number of distinct tasks.

More recently, a few methods such as AutoML-Zero (Real et al., 2020) and XD-operations (Roberts et al., 2021) have been introduced to relax the biases encoded by standard search spaces to enable more general applicability in theory. However, the former was not designed for practical deployment, and while XD achieves good predictive accuracy on a handful of interesting problems, it is too computationally demanding for practical usage (c.f. Fig. 1b). Hence we ask: is there an approach that can provide sufficient expressivity and multi-domain capability while still retaining the faster search and the more efficient final models of discrete architecture search?

In this work, we answer in the affirmative by introducing **DASH** (**D**iverse-task **A**rchitecture **S**earc**H**), a NAS method that adapts standard CNN backbones to various learning problems by finding substitutes for their layer operations (*multi-domain capability*), and does so using the continuous relaxation and discretization pipeline to speed up search and retraining (*efficiency*). This approach is inspired by the success of XD-operations on accuracy metrics, which suggests that replacing certain layers in a CNN with new operations can be sufficient for solving diverse tasks. To maintain efficiency, we restrict DASH’s search space to a discrete set of named operations, as opposed to the XD approach of considering a parametrized space with infinitely many operations that can be continuously evolved.

Concretely, we consider a search space of cross-scale convolutions that contains operators with filters covering a wide range of kernel sizes and dilations. The motivation is straightforward: previous work has exemplified the effectiveness of dilated convolutions in multi-scale feature extraction (van den Oord et al., 2016; Yang et al., 2017) and context aggregation (Yu & Koltun, 2016; Chen et al., 2018b) for tasks in different domains. We highlight the inclusion of large filters in our search space. In particular, large kernel sizes are critical to dense prediction (Peng et al., 2017) and can resemble global-attention in Transformers (Liu et al., 2022), whereas large dilations are capable of modeling long-range dependencies (Bai et al., 2018; 2019).

Despite its usefulness, existing NAS search spaces have largely ignored varying filter sizes and dilation rates beyond one or two settings each (Liu et al., 2019b). One likely cause is the assumed sufficiency of small kernels on typical tasks studied by the community, e.g., image classification. A more crucial concern is computational complexity, as the cost of popular weight-sharing methods scales directly with the number of operations considered and quadratically with the largest kernel size. We overcome the obstacles and develop a practical method for exploring multi-scale convolutions via three techniques. The first two exploit mathematical properties of convolutions. The last one takes advantage of fast matrix multiplication on GPUs. Specifically:

1. Using the **linearity** of convolutions, we mix several convolutions by computing one convolution equipped with a combined kernel rather than applying each filter separately and aggregating multiple outputs. While the number of convolution computations required by the naive aggregation of $|K|$ possible kernel sizes and $|D|$ possible dilations is $\mathcal{O}(|K||D|)$, our approach has $\mathcal{O}(1)$ complexity, independent of the search space size.
2. Using the **diagonalization** of convolutions, we relegate a major portion of the computation to element-wise multiplication in the Fourier domain, minimizing the effect of the largest kernel size on the computational complexity

of our algorithm. For instance, a standard 1D convolution requires $\mathcal{O}(nk)$ operations to convolve a kernel of size k with a length- n input. Yet a Fourier convolution takes only $\mathcal{O}(n \log n)$, a critical improvement that makes searching over large kernels significantly easier.

3. Our final strategy is to use Kronecker products of undilated kernels and small sparse matrices to compute dilated kernels quickly on GPUs. This brings an additional two-fold speedup on top of the previous techniques.

In our work, we analyze the asymptotic complexity of the first two techniques and verify the practical utility when all three are combined together. The resulting algorithm, DASH, achieves a ten-fold speedup for differentiable NAS over the multi-scale search space. Aside from these innovations, DASH employs the standard weight-sharing scheme of training a supernet, discretizing to obtain a model, and retraining the selected model for end tasks (Liu et al., 2019b).

We evaluate DASH on NAS-Bench-360 (Tu et al., 2021), a benchmark containing a suite of ten datasets that span multiple application areas such as PDE-solving, disease prediction, and protein folding. As shown in Fig. 1a, DASH yields models with better aggregate performance than those returned by leading AutoML methods as well as hand-designed, task-specific architectures. As for individual tasks, DASH beats all past automated approaches on seven of the ten problems and exceeds hand-designed models on six, simultaneously maintaining strong efficiency relative to existing weight-sharing methods like DARTS (c.f. Fig. 1b). Our code is made public at <https://github.com/sjunhongshen/DASH>.

2. Related Work

Neural architecture search (NAS) aims to automate neural network design. Most methods have two components: a search space of proper architectures and a search algorithm that finds models. There has been significant progress in both search space design (Zoph et al., 2018; Liu et al., 2019b; Roberts et al., 2021) and search strategy development (Pham et al., 2018; Liu et al., 2019b; Xie et al., 2019; Xu et al., 2020; Li et al., 2021a). In this work, we focus on improving task diversity through a novel search space. Our search algorithms are largely borrowed from prior work.

According to Elsken et al. (2019), the search space can be decomposed into a set of micro layer operators and the macro rules that define the high-level topology of the network. Three types of widely used NAS search spaces are cell-based (Pham et al., 2018; Real et al., 2019), hierarchical (Liu et al., 2018a;b), and morphism-based (Chen et al., 2016; Wei et al., 2016). Our method belongs to the last category, as we generate new architectures from existing CNN backbones. We specifically focus on expanding the opera-

tion space to multiple types of convolutions, simultaneously varying the kernel size and the dilation factor. Past work has at most studied the easier problem of altering dilation alone, and only for vision tasks (Chen et al., 2018a).

NAS is often evaluated on image classification (Liu et al., 2019b) or semantic segmentation (Chen et al., 2018a). There has been some effort to diversify to settings such as image restoration (Suganuma et al., 2018), audio classification (Mehrotra et al., 2021), and machine translation (So et al., 2019), but problems beyond these popular domains are less-explored. A few recent works have begun to study more diverse tasks (Zela et al., 2020; Roberts et al., 2021), and we make use of a new benchmark, NAS-Bench-360, that was introduced for the same purpose (Tu et al., 2021).

2.1. Differentiable Architecture Search (DARTS)

In this work, we seek to fuse strong aspects of two NAS methods: the efficiency of DARTS (Liu et al., 2019b) and the expressivity of XD-operations (Roberts et al., 2021). The former introduces the continuous relaxation scheme to the weight-sharing paradigm (Pham et al., 2018) and enables us to gain information about many networks by training one combined supernet. Concretely, DARTS relaxes the discrete choice of operations at each edge in a computational graph as a softmax, enabling the search process to be end-to-end differentiable and amenable to regular optimizers. After search, it discretizes the softmax weights based on their magnitudes to output a valid architecture.

Despite its efficiency, DARTS has limited operator diversity: its search space contains only eight operations, of which just four convolutions are parameterized. While this might be enough for some vision tasks, it has been shown that the DARTS search space is insufficient for inputs other than low-resolution images, e.g., time-series (Tu et al., 2021). At the same time, the simplest approach for expanding the search set—adding operations one-by-one—scales poorly, as reflected in the small operation spaces of similar methods such as DenseNAS (Fang et al., 2020) and AMBER (Zhang et al., 2021). For example, AMBER simply shifts the kernel size up for good performance on long-sequence genomic data. Yet the significantly superior results of DASH on such datasets show that we should instead consider more convolutions with different receptive field sizes rather than a few large ones. Hence, in this paper, we study how to increase the number of convolutions that a DARTS-like supernet can handle while maintaining practical efficiency.

Specifically, given multiple convolutions as the incoming operations at a node, DARTS computes each convolution separately and outputs the aggregated result to the next node. An alternative approach is to take advantage of the linearity of convolutions—we can first mix the kernels and then apply convolution once. This kernel-mixing strategy, which we

call *mixed-weights* and will define formally later, has been employed by MergeNAS (Wang et al., 2020) and RepVGG (Ding et al., 2021) to improve search and inference speed, respectively. It works well for *a few small* kernels. However, we will show that *mixed-weights* on its own is insufficient for searching over *many large* kernels, i.e., a diverse kernel set that is crucial for solving diverse problems. Hence, other techniques are needed to overcome the efficiency bottleneck.

2.2. Expressive Diagonalization (XD) Operations

The second work we build upon is XD-operations (Roberts et al., 2021), which targets a much more expansive search space containing infinitely many operations, including all types of convolutions, average pooling, skip-connections, graph convolutions (Kipf & Welling, 2017), and FNOs (Li et al., 2021b). To construct the search space, Roberts et al. (2021) expresses the convolution operation acting on input x with filter w using the convolution theorem, i.e., $\text{Conv}(w)(x) = K \text{diag}(Lw)Mx$, where K, L, M are appropriate discrete Fourier transforms (DFTs). A richer operation space is then obtained by allowing these transforms to take on a general class of fast matrices (Dao et al., 2020). Compatible with gradient-based optimization methods, XD demonstrates strong performance on new tasks such as PDE solving and protein folding. However, its search process requires an unacceptably long time and large memory (Fig. 1b), and the resulting architectures are as inefficient as the supernet due to the absence of a discretization step. We thus seek to combine the continuous relaxation of DARTS with a discretized variant of XD to obtain a new operation space that is not only more expressive than the former but also more efficient than the latter.

3. Methods

Now, we describe the details of DASH (Algorithm 1). We first explain how DASH leverages existing networks to initialize the supernet and generate different models for diverse tasks. Then, we formally define the multi-scale convolution search space and propose a fast way to search this space using the three efficiency-motivated techniques mentioned earlier. Finally, we outline the procedure for discretizing the search space and retraining the searched model.

3.1. Decoupling Topology and Operations

Every architecture is a mapping from model weights to functions and can be described by a directed acyclic graph $G(V, E)$. Each edge in E is characterized by (u, v, Op) , where $u, v \in V$ are nodes and Op is an operation applied to u . Node v aggregates the outputs of its incoming edges. NAS aims to automatically select the edge operations and the graph topology to optimize some objective. For each edge in E , Op is chosen from a search space

$S = \{\mathbf{Op}_a \mid a \in A\}$ where $a \in A$ are architecture parameters. In past work, A usually indexes a small set of operations. For instance, the DARTS search space specifies $A_{discrete} = \{1, \dots, 8\}$ with the operations being **Zero**, **Id**, **MaxPool**_{3×3}, **AvgPool**_{3×3}, **Conv**_{3×3}, **Conv**_{5×5}, **DilatedConv**_{3×3,2}, and **DilatedConv**_{5×5,2}. However, A can also be defined systematically to identify key properties of the operators, e.g., $A = \{\text{convolutions with many (kernel size, dilation rate) pairs}\}$, as we will discuss shortly.

A common approach to determine the topology of the output network is to search for blocks of operations and stack several blocks together. In this work, we take a different route that is similar to [Roberts et al. \(2021\)](#): we use existing networks as backbones and replace certain layers in the backbone with the searched operations. Specifically, we select a set of architectures to accommodate both 1D and 2D datasets. Convolutional layers with different kernels can then be plugged into these networks to achieve multi-resolution models. An advantage of decoupling topology and operation search is flexibility: the searched operators can vary from the beginning to the end of a network, so features at different granularities can be processed differently.

For our backbone networks, we pick Wide ResNets (WRNs) ([Zagoruyko & Komodakis, 2016](#); [Fawaz et al., 2020](#)) for both 2D and 1D tasks due to its simplicity and effectiveness in image and sequence modeling. Before search, the supernet is initialized to the backbone. To find operators for cross-scale features, we substitute all **Conv** layers with a new operator **AggConv** _{K,D} (short for aggregated convolution) that represents the new search space which we now define. For simplicity, our mathematical discussion in the following will stick to the 1D case, although our experiments are on both 1D and 2D data.

3.2. Efficiently Searching for Multi-Scale Convolutions

A convolution filter is mainly specified by two hyperparameters, the kernel size k and the dilation rate d (we do not consider stride which does not change the filter shape). The effective filter size is $(k-1)d+1$ with nonzero entries separated by $d-1$ zeros. Given input data with shape n , let K be our interested set of kernel sizes, D the set of dilations.

Let **Conv** _{k,d} be the convolution operation with kernel size k , dilation rate d , c_{in} input channels, and c_{out} output channels. We will define the **AggConv** _{K,D} search space as

$$S_{\text{AggConv}_{K,D}} = \{\mathbf{Conv}_{k,d} \mid k \in K, d \in D\}. \quad (1)$$

Hence, $A = K \times D$ in previous notations. $S_{\text{AggConv}_{K,D}}$ contains a collection of convolutions with receptive field size ranging from k_{min} to $d_{max}(k_{max}-1)+1$, which allows us to discover models that process the input with varying resolution and coverage at each stage.

Algorithm 1 DASH

Input: training data Z , loss function l , set of kernel sizes K , set of dilation rates D , subsampling ratio p
 Initialize the backbone
 Replace each **Conv** layer with mixed op **AggConv** _{K,D}
while not converged **do**
 Subsample $p|Z|$ training points uniformly at random
 Compute forward pass using Equation 4
 Descend architecture parameters α by $\nabla_\alpha l(\mathbf{w}, \alpha)$
 Descend model weights \mathbf{w} by $\nabla_{\mathbf{w}} l(\mathbf{w}, \alpha)$
end while
 Select $\arg \max_{k \in K, d \in D} \alpha_{k,d}$ for each **AggConv** layer
 Tune retraining hyperparameters on a validation subset
 Retrain the discretized model with all training data

To retain the efficiency of discrete NAS, we apply the continuous relaxation scheme of DARTS to $S_{\text{AggConv}_{K,D}}$, which mixes all operations in the space using architecture parameters $\{\alpha_{k,d} \in \Delta_{|K||D|} \mid (k, d) \in K \times D\}$ ¹, so the output of each edge in the computational graph is

$$\text{AggConv}_{K,D}(\mathbf{x}) := \sum_{k \in K} \sum_{d \in D} \alpha_{k,d} \cdot \mathbf{Conv}(\mathbf{w}_{k,d})(\mathbf{x}). \quad (2)$$

Here $\{\mathbf{w}_{k,d} \mid (k, d) \in K \times D\}$ are the kernel weights for each operation being considered. The resulting supernet can be trained end-to-end, and our hope is that after search, the most important operation is assigned the highest weight. However, the complexity of computing the above summation directly, a baseline algorithmic approach we call **mixed-results**, is $\mathcal{O}(c_{in}c_{out}(|K||D| + \bar{K})n)$, where $\bar{K} := |D| \sum_{k \in K} k$. **mixed-results** can be very expensive when we increase the maximum element in K or D with larger input size n . To improve upon it, we propose three techniques which build up to the efficiency-oriented DASH.

TECHNIQUE 1: MIXED-WEIGHTS

Since convolution is linear, instead of computing $|K||D|$ convolutions, we can combine the kernels and compute convolution once as [Wang et al. \(2020\)](#); [Ding et al. \(2021\)](#) do. We call this approach **mixed-weights**:

$$\text{AggConv}_{K,D}(\mathbf{x}) = \mathbf{Conv} \left(\sum_{k \in K} \sum_{d \in D} \alpha_{k,d} \cdot \mathbf{w}'_{k,d} \right) (\mathbf{x}). \quad (3)$$

Here \mathbf{w}' is the properly padded version of \mathbf{w} so that filters of different sizes can be added. The aggregated kernel has size $\bar{D} := \max_{k,d} (k-1)d+1$ and the n -dependent term of the complexity of **mixed-weights** is $c_{in}c_{out}\bar{D}n$. Hence, it removes the direct dependence of the leading-order term on $|K||D|$, the search space size, that **mixed-results** had.

¹ Δ denotes the probability simplex.

Table 1: Complexity of different methods for computing AggConv . For notation, $\bar{K} := |D| \cdot \sum_{k \in K} k$, $\bar{D} := \max_{k,d} (k-1)d + 1$. A detailed analysis is provided in Appendix B.

Method	MULTs	ADDs
<i>mixed-results</i> (Equation 2)	$(c_{in}c_{out}\bar{K} + c_{out} K D)n$	$(c_{in}c_{out}\bar{K} + c_{out} K D)n$
<i>mixed-weights</i> (Equation 3)	$c_{in}c_{out}(\bar{K} + \bar{D}n)$	$c_{in}c_{out}\bar{D}(K D + n)$
DASH (Equation 4)	$c_{in}c_{out}(\bar{K} + n) + \mathcal{O}(c_{in}c_{out}n \log n)$	$c_{in}c_{out}(K D \bar{D} + n) + \mathcal{O}(c_{in}c_{out}n \log n)$

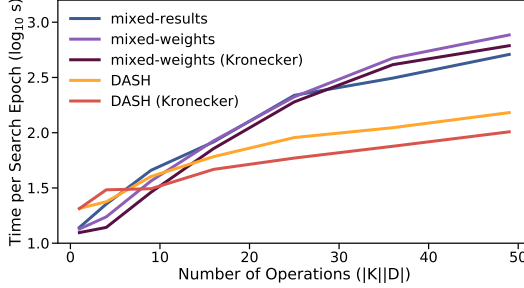


Figure 2: \log_{10} time for one search epoch vs. number of operations in $S_{\text{AggConv}_{K,D}}$ evaluated on 1D input. We vary the search space by letting $K = \{2p + 1 | 1 \leq p \leq c\}$, $D = \{2^q - 1 | 1 \leq q \leq c\}$ and increasing c from 1 to 7.

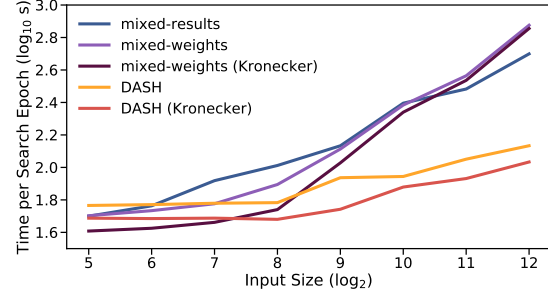


Figure 3: \log_{10} time for one search epoch vs. input size of 1D data. We fix $K = \{3, 5, 7, 9, 11\}$, $D = \{1, 3, 7, 15, 31\}$ and test $n \in \{2^5, \dots, 2^{12}\}$.

TECHNIQUE 2: FOURIER CONVOLUTION

If we wish to increase the kernel size and dilation with the input size, the complexity of *mixed-weights* will still grow *implicitly* with the search space size through the dependence on \bar{D} . To address this issue, we combine the kernel re-weighting idea with another technique motivated by the convolution theorem. Given a kernel \mathbf{w} , recall that $\text{Conv}(\mathbf{w})(\mathbf{x}) = \mathbf{F}^{-1} \text{diag}(\mathbf{F}\mathbf{w}')\mathbf{F}\mathbf{x}$, where \mathbf{F} is the discrete Fourier transform (DFT) and $\text{diag}(\mathbf{z})$ is a diagonal matrix with entries \mathbf{z} . In other words, convolution involves multiplying the FFT of the kernel by that of the input. Since the DFT can be applied in time $\mathcal{O}(n \log n)$ using the Fast Fourier Transform (FFT) and apart from that we only need element-wise multiplication, this yields an efficient approach to reducing dependence on the combined kernel size \bar{D} . The use of the convolution theorem is inspired by Roberts et al. (2021), who replaced the FFTs with a continuous set of matrices for XD-operations. Indeed, our search space may be viewed mathematically as a replacement of the middle DFT by a *discrete* set of matrices. However, while their motivation was expressivity, ours is efficiency.

Accordingly, DASH computes $\text{AggConv}_{K,D}$ as follows:

$$\begin{aligned} \text{AggConv}_{K,D}(\mathbf{x}) \\ = \mathbf{F}^{-1} \text{diag} \left(\mathbf{F} \left(\sum_{k \in K} \sum_{d \in D} \alpha_{k,d} \cdot \mathbf{w}'_{k,d} \right) \right) \mathbf{F}\mathbf{x}. \end{aligned} \quad (4)$$

Note that while the kernel changes for each $\text{Conv}_{k,d}$, the input does not. Hence, we also save time by transforming the input to the frequency domain only once.

In Table 1, we report the theoretical complexities of the baselines and DASH, the latter leveraging both Technique 1 and 2. It is easy to obtain the operation complexities of *mixed-weights* and *mixed-results*. For DASH, the number of multiplications and additions can be attributed to the inner weight sum and multi-channel product (the first term) as well as three FFTs (the second). A detailed analysis is provided in Appendix B. We see that *mixed-weights* is favorable to *mixed-results* when $\bar{D} < \bar{K} = \mathcal{O}(|D|k_{\max}^2)$, which occurs with large kernels and a few dilations. On the other hand, only DASH completely separates the dominant terms containing $c_{in}c_{out}n$ from the size of the search space and its elements, replacing them by $\mathcal{O}(\log n)$, which is small for any realistic n . As we increase k_{\max} and d_{\max} for larger inputs, this will also lead to a slower asymptotic increase in complexity, making DASH an attractive choice for the multi-scale search space where \bar{D} is large by design to extract possible long-range dependencies in the data.

TECHNIQUE 3: KRONECKER DILATION

To efficiently implement the kernel summation in *mixed-weights* and DASH on a GPU, we introduce our final technique: after initializing $\mathbf{w}_{k,d}$ for each $\text{Conv}_{k,d}$ separately, we use a Kronecker product \otimes to transform the undilated kernels into dilated forms. For example, to compute a 2D

convolution with dilation d , we introduce the sparse pattern matrix $\mathbf{P} \in \mathbb{R}^{d \times d}$ such that $\mathbf{w}_{k,d} = \mathbf{w}_{k,1} \otimes \mathbf{P}$:

$$\mathbf{P} = \begin{bmatrix} 1 & 0 & \cdots & 0 \\ 0 & 0 & \cdots & 0 \\ \vdots & \vdots & \ddots & \vdots \\ 0 & 0 & \cdots & 0 \end{bmatrix} \quad (5)$$

Apart from the theoretical gains in Wu et al. (2019), we show that this way of dilating the kernels is empirically faster than the standard way of padding 0's into $\mathbf{w}_{k,1}$ (Fig. 2 and 3). After dilating the kernels, we sum them together, zero-pad to match the input size, and apply the FFTs.

To check that our asymptotic analysis leads to actual speedups and perform an ablation study on the proposed techniques, we evaluate the three methods on single-channel 1D input (experiment details are in Appendix C). Since both *mixed-weights* and DASH require kernel summation, which can be implemented with Kronecker dilation (Technique 3), we compare five methods in total. Fig. 2 illustrates the combined forward and backward pass time in log scale for one search epoch vs. the size of $S_{\text{AggConv}_{K,D}}$ when $n = 1000$. For small \bar{D} , the difference is negligible. However, as \bar{D} increases, the DASH curves grow slowly whereas the runtimes for the other methods scale with the number of operations.

In Fig. 3, we fix K and D to study how runtime is affected by input size n . Both *mixed-results* and *mixed-weights* become extremely inefficient for large n 's which commonly occur in time-series or signal processing. Surprisingly, DASH's runtime does not increase much with n . We hypothesize that this is due to wallclock-time being dominated by data-passing at that speed. In general, Kronecker dilation contributes to $2 \times$ speedups for *mixed-weights* and DASH. As shown in Fig. 2 and 3, DASH (Kronecker) results in approximately $10 \times$ speedups for search compared to *mixed-results* in both the large operation space and large input size regimes. Hence, we use this version of DASH in our experiments.

3.3. The Full Pipeline: Architecture Search, Hyperparameter Optimization, and Retraining

Having shown the main techniques for searching a large space of kernel patterns, we now detail our NAS method, i.e., the exact search and model development pipeline.

Given a dataset, we set $K = \{3 + d(p-1) | 1 \leq p \leq p_{\max}\}$ for kernel sizes and $D = \{2^q - 1 | 1 \leq q \leq q_{\max}\}$ for dilations. For 2D input, we set d to 2, p_{\max} to 4, and q_{\max} to 4. For relatively long 1D sequence data, we have $d = 4$, $p_{\max} = 5$, and $q_{\max} = 4$. For instance, CIFAR has size $3 \times 32 \times 32$ where 3 is the number of channels and $n = 32$. The corresponding K is $\{3, 5, 7, 9\}$ and D is $\{1, 3, 7, 15\}$. To normalize architecture parameters into a probability distribution over operations, we adopt the soft

Gumbel Softmax activation, similar to Xie et al. (2019).

The backbone networks are as follows. For 2D tasks, we use WRN 16-1 with depthwise-separable convolutions as the search backbone to accelerate supernet training. We use WRN 16-4 with regular convolutions for retraining. For 1D tasks, we use 1D WRN (Fawaz et al., 2020) in the entire pipeline. During search, we subsample the training data at each epoch. Given the loss for the target task, DASH jointly optimizes the model weights and the architecture parameters. This single-level optimization is more efficient than two-stage NAS, which finds initial assignments for architecture parameters and trains the candidates from scratch.

After searching for a predefined number of epochs, we discretize the search space and pick $\mathbf{Conv}_{k,d} \in S_{\text{AggConv}_{K,D}}$ with the largest weight for each layer. The final model has a similar overall structure to the backbone, but the operations performed at the intermediate layers are tailored to the specific task of interest. To improve training stability, we additionally add a simple hyperparameter tuning stage between search and retraining using grid search and early stopping. As we use the SGD optimizer and WRN contains dropout layers, the configuration space is as follows:

Learning rate	$\{1e-1, 1e-2, 1e-3\}$
Weight decay	$\{5e-4, 5e-6\}$
Momentum	$\{0.9, 0.99\}$
Dropout rate	$\{0, 0.05\}$

For each hyperparameter setting, we train a discretized model on a subset of the training data for some epochs and evaluate the model's performance on a holdout validation set. Then, we select the configuration with the highest validation accuracy. As a final step, we retrain the discretized model with the optimal hyperparameters on the entire training set for downstream applications. Like other weight-sharing methods with discretization, our final architecture will be more efficient than the supernet.

4. Evaluation

We evaluate the performance of DASH on diverse tasks using NAS-Bench-360 (Tu et al., 2021), a benchmark of ten tasks spanning multiple application domains, input dimensions, and learning objectives.² These include classical vision tasks such as CIFAR-100 where CNNs do well, scientific computing tasks such as Darcy Flow where standard CNN backbones can perform poorly (Li et al., 2021b; Roberts et al., 2021), sequence tasks such as DeepSEA where large dilations are preferred (Bai et al., 2018; Zhang et al., 2021), and many others. Thus, our evaluation will not only test whether DASH can find good architectures in the proposed

²For completeness, we give a task summary in the Appendix.

Table 2: Accuracy results on NAS-Bench-360 tasks. The last three problems are 1D and the rest are 2D. Methods are grouped into three classes: non-automated, automated, and the DASH family. Scores of DASH are averaged over three trials. Scores of the baselines are from Tu et al. (2021). See Table 5 in the Appendix for standard deviations.

	CIFAR-100 0-1 error ^l	Spherical 0-1 error ^l	Darcy Flow relative ℓ_2 ^l	PSICOV MAE ₈ ^l	Cosmic FNR ^l	NinaPro 0-1 error ^l	FSD50K mAP ^h	ECG F1 ^h	Satellite 0-1 error ^l	DeepSEA AUROC ^h
Expert	19.39	67.41	0.008	3.35	25.29	8.73	0.38	0.72	19.8	0.70
WRN	23.35	85.77	0.073	3.84	51.76	6.78	0.08	0.57	15.49	0.60
TCN	-	-	-	-	-	-	-	0.43	16.21	0.56
WRN-ASHA	23.39	75.46	0.066	3.84	37.53	7.34	0.09	0.57	15.84	0.59
DARTS-GAEA	24.02	48.23	0.026	2.94	31.15	17.67	0.06	0.66	12.51	0.64
DenseNAS	25.98	72.99	0.10	3.84	79.52	10.17	0.36	0.60	13.81	0.60
Auto-DL	-	-	0.049	6.73	99.79	-	-	-	-	-
AMBER	-	-	-	-	-	-	-	0.67	12.97	0.68
BABY DASH	25.56	68.55	0.016	3.94	13.18	8.28	0.38	0.63	13.29	0.63
DASH	24.37	75.44	0.0079	3.30	15.04	6.60	0.40	0.68	12.28	0.72

^{h/l} a higher / lower value of the metric indicates better performance.

new search space, but also investigate whether multi-scale convolution is a strong competitor for solving different problems. In fact, our results show that DASH is a top choice for many tasks, obtaining in-aggregate the best speed-accuracy trade-offs among the methods we evaluate (c.f. Fig. 5).

4.1. Baselines and Competitor Methods

For each NAS-Bench-360 task, we compare DASH with the following methods: DenseNAS (Fang et al., 2020) and GAEA PC-DARTS (Li et al., 2021a), which represent general NAS; Auto-DeepLab (Liu et al., 2019a) and AMBER (Zhang et al., 2021), which represent specialist NAS methods for dense prediction and 1D tasks, respectively; 1D temporal convolutional network (TCN) (Bai et al., 2018), regular WRN, and WRN with hyperparameter tuner ASHA (Li et al., 2020), which represent natural NAS baselines.

While the results of the above methods are available in Tu et al. (2021), we additionally add a BABY DASH baseline: we run DASH in the DARTS convolution space by setting $K = \{3, 5\}$ and $D = \{1, 2\}$ to study whether large kernel sizes and dilations are necessary to strong performance across-the-board. Finally, we compare our method to the expert architectures selected by NAS-Bench-360. These models are representatives of the best that hand-crafting currently has to offer.

4.2. Experimental Setup

Each dataset is preprocessed and split using the NAS-Bench-360 script, with the training set used for search, hyperparameter tuning, and retraining. To construct the multi-scale search space, we set K and D according to the rules in Section 3.3. As discussed previously, we perform single-level

optimization during the search process, simultaneously updating the shared weights and architecture parameters. We use the default SGD optimizer for the WRN backbone and fix the learning rate schedule as well as the gradient clipping threshold for every task. The entire DASH pipeline can be run on a single NVIDIA V100 GPU, which is also the system that we use to report the runtime cost. Full experimental details can be found in the Appendix.

We evaluate the performance of all competing methods following the NAS-Bench-360 protocol. We first report results of the target metric for each task by running the model of the *last* epoch on the test data. Then, we report aggregate results via *performance profiles* (Dolan & Moré, 2002), a technique that considers both outliers and small performances differences to compare methods across multiple tasks robustly. In such plots, each curve represents one method. The τ on the x -axis denotes the fraction of tasks on which a method is no worse than a τ -factor from the best.

4.3. Results and Discussion

We present the accuracy results for each task in Table 2 and the performance profiles in Fig. 4. Fig. 4 clearly demonstrates that DASH is superior to other competing methods in terms of aggregate performance. In particular, it achieves top performance for 6/10 tasks, ranks first among all *automated* models for 7/10 tasks, and performs favorably when considering both accuracy and efficiency as shown in Fig. 5. In addition, Table 3 shows that DASH outperforms DARTS in speed for all 10 tasks (in several cases by an order of magnitude), and attains comparable efficiency with vanilla WRN for 6/10 tasks (full-pipeline time is less than or about twice as long as the WRN training time). In the following, we provide a detailed analysis of the experimental results.

Table 3: Full-pipeline runtime in GPU hours for NAS-Bench-360. Results for DARTS, DenseNAS, and WRN are taken from Tu et al. (2021). Runtime breakdown for DASH is provided in Appendix G. PSICOV results are omitted due to a discrepancy in the implementation of data processing.

Task	DARTS	DenseNAS	WRN	DASH
CIFAR-100	9.5	2.5	2	2.5
Spherical	16.5	2.5	2	5
Darcy Flow	6.5	0.5	0.5	5.3
Cosmic	21.5	2.5	4	6.8
NinaPro	0.5	0.2	0.2	0.3
FSD50K	37	4.5	4	29
ECG	140	6.5	5	1.3
Satellite	28	3	4.5	6.5
DeepSEA	39.5	2	1.5	10

DASH dominates automated methods. Compared to other automated methods, DASH has a clear advantage in accuracy. Even for tasks where it does not beat the expert, e.g. ECG, DASH’s performance is significantly better than other AutoML methods. It also outperforms specialist methods Auto-DL and AMBER on dense prediction and 1D tasks, respectively. Although DARTS does best on CIFAR-100 (the task for which it was designed), Spherical, and PSICOV, it is the worst on NinaPro and FSD50K. Note that the under-performance of DASH on CIFAR-100 relative to WRN (and on Spherical and Cosmic relative to BABY DASH) suggests suboptimality of the search algorithm but not of the operation space, since WRN (and BABY DASH) is contained in our search space. This suggests significant scope to improve search over the DASH operation space.

DASH dominates expert architectures. While the degree of sophistication of the expert networks varies task by task (Tu et al., 2021), the performance of DASH on tasks such as Darcy Flow suggests that it is capable of competing with highly specialized networks, e.g., the specially designed Fourier Neural Operator (Li et al., 2021b) for PDE solving. These results imply that DASH, and more generally the strategy of equipping backbone networks with learned task-specific kernels, is a promising approach for tackling model development for new tasks.

Large kernels are useful. We investigate whether multi-scale convolutions are essential for solving specific types of tasks by comparing DASH with BABY DASH, as motivated earlier. We hypothesize that for the same task, a small performance gap between the two methods would indicate that small kernels suffice for extracting local features, whereas a major degrade in the quality of the BABY DASH model can imply that the task needs global modeling. Consequently,

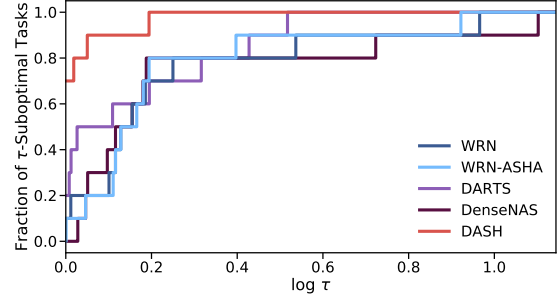


Figure 4: Performance profiles of general NAS methods and DASH on NAS-Bench-360. DASH being far in the top left corner indicates it is rarely suboptimal and is often the best.

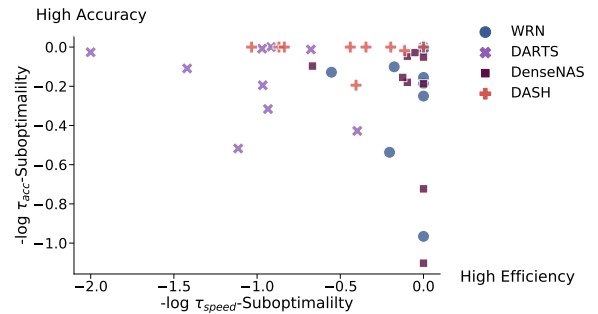


Figure 5: Scatterplot comparing $-\log \tau$ -suboptimality of speed vs. accuracy on all tasks. DASH’s concentration in the top right corner indicates its strong efficacy-efficiency trade-offs relative to the other methods.

datasets such as Darcy Flow and ECG provide compelling evidence that kernels with large receptive fields play an important role in solving real-life problems and further back up the design of our search space.

DASH is computationally efficient. In addition to prediction quality, we also care about the efficiency of model selection. Table 3 provides the combined search and retraining time in GPU hours for DARTS, DenseNAS, and DASH, as well as the training time for vanilla WRN 16-4 (without hyperparameter tuning). We also present the breakdown of DASH’s full-pipeline runtime in Appendix G. A key observation is that the cost of DASH is consistently below DARTS’s on all tasks and is similar to training a simple CNN for more than half of them. Although DenseNAS stands out by speed, its practical performance is less impressive.

In Fig. 5, we visualize the trade-off between efficiency and effectiveness for each method and task combination. Evidently, DASH takes an important step towards bridging the gap between the efficiency of DARTS and the expressivity of XD in NAS. The fact that DASH can be trained at a low cost testifies that we need not sacrifice efficiency for adding more operations. In fact, we have actually shown that DASH is *both* faster *and* more effective than DARTS in many tasks.

4.4. Limitations and Future Work

There are several open problems which we leave for future work. First, it is beneficial to study why certain kernel patterns are chosen, as the selected operations can hint us at the intrinsic properties of the datasets. Second, although this paper focuses on NAS, which is an alternative to fine-tuning pre-trained models, the aggregated convolution can be a plug-and-play module for algorithms that search for large-scale models. Third, one can improve upon DASH itself, e.g. by including non-square convolutions in the 2D case or combining it with a better search algorithm. More ambitiously, one could construct a more comprehensive search space containing high-level operators such as BatchNorm and self-attention or use other backbones such as ConvNeXt (Liu et al., 2022). Finally, lowering the barrier for applying ML necessarily comes with the risk of misuse. Hence, it is imperative to develop NAS methods with privacy and fairness guarantees, which goes beyond the objective that DASH currently uses.

5. Conclusion

In this paper, we argue that a crucial goal of NAS is to discover accessible models for diverse tasks. To this end, we propose DASH, which efficiently searches for convolution patterns and integrates them into existing backbones. DASH overcomes the computational limitations of differentiable NAS and obtains high-quality models with accuracy comparable to or better than that of the handcrafted networks on many tasks. Our experiments show that convolution can be a universal operator for many under-explored areas. DASH is also a promising first step towards developing general-purpose models with more complicated structure.

Acknowledgments

We thank Maria-Florina Balcan, Nicholas Roberts, and Renbo Tu for providing useful feedback. This work was supported in part by DARPA FA875017C0141, the National Science Foundation grants IIS1705121, IIS1838017, IIS2046613 and IIS-2112471, an Amazon Web Services Award, a Facebook Faculty Research Award, funding from Booz Allen Hamilton Inc., a Block Center Grant, and a Facebook Fellowship Award. Any opinions, findings and conclusions or recommendations expressed in this material are those of the author(s) and do not necessarily reflect the views of any of these funding agencies.

References

Adhikari, B. DEEPCON: protein contact prediction using dilated convolutional neural networks with dropout. *Bioinformatics*, 36(2):470–477, 07 2019.

Bai, S., Kolter, J. Z., and Koltun, V. An empirical evaluation of generic convolutional and recurrent networks for sequence modeling. *arXiv*, 2018.

Bai, S., Kolter, J. Z., and Koltun, V. Trellis networks for sequence modeling. In *Proceedings of the 7th International Conference on Learning Representations*, 2019.

Chen, L.-C., Collins, M. D., Zhu, Y., Papandreou, G., Zoph, B., Schroff, F., Adam, H., and Shlens, J. Searching for efficient multi-scale architectures for dense image prediction. In *Advances in Neural Information Processing Systems*, 2018a.

Chen, L.-C., Papandreou, G., Kokkinos, I., Murphy, K. P., and Yuille, A. L. Deeplab: Semantic image segmentation with deep convolutional nets, atrous convolution, and fully connected crfs. *IEEE Transactions on Pattern Analysis and Machine Intelligence*, 40:834–848, 2018b.

Chen, T., Goodfellow, I. J., and Shlens, J. Net2net: Accelerating learning via knowledge transfer. 2016.

Cohen, T., Geiger, M., Köhler, J., and Welling, M. Spherical cnns. In *International Conference on Machine Learning*, 2018.

Dao, T., Sohoni, N., Gu, A., Eichhorn, M., Blonder, A., Leszczynski, M., Rudra, A., and Ré, C. Kaleidoscope: An efficient, learnable representation for all structured linear maps. In *Proceedings of the 8th International Conference on Learning Representations*, 2020.

Dempster, A., Petitjean, F., and Webb, G. I. Rocket: exceptionally fast and accurate time series classification using random convolutional kernels. *Data Mining and Knowledge Discovery*, 34:1454–1495, 2020.

Ding, X., Zhang, X., Ma, N., Han, J., Ding, G., and Sun, J. Repvgg: Making vgg-style convnets great again. 2021 *IEEE/CVF Conference on Computer Vision and Pattern Recognition (CVPR)*, pp. 13728–13737, 2021.

Dolan, E. D. and Moré, J. J. Benchmarking optimization software with performance profiles. *Mathematical Programming*, 91:201–213, 2002.

Elsken, T., Metzen, J. H., and Hutter, F. Neural architecture search: A survey. *Journal of Machine Learning Research*, 20(55):1–21, 2019.

Fang, J., Sun, Y., Zhang, Q., Li, Y., Liu, W., and Wang, X. Densely connected search space for more flexible neural architecture search. In *Proceedings of the IEEE Conference on Computer Vision and Pattern Recognition*, 2020.

Fawaz, H. I., Lucas, B., Forestier, G., Pelletier, C., Schmidt, D. F., Weber, J., Webb, G. I., Idoumghar, L., Muller, P.-A., and Petitjean, F. Inceptiontime: Finding alexnet for time series classification. *Data Mining and Knowledge Discovery*, 34:1936–1962, 2020.

Fonseca, E., Favory, X., Pons, J., Font, F., and Serra, X. Fsd50k: an open dataset of human-labeled sound events. *ArXiv*, abs/2010.00475, 2021.

Hong, S., Xu, Y., Khare, A., Priambada, S., Maher, K. O., Aljiffry, A., Sun, J., and Tumanov, A. Holmes: Health online model ensemble serving for deep learning models in intensive care units. *Proceedings of the 26th ACM SIGKDD International Conference on Knowledge Discovery & Data Mining*, 2020.

Huang, G., Liu, Z., and Weinberger, K. Q. Densely connected convolutional networks. *2017 IEEE Conference on Computer Vision and Pattern Recognition (CVPR)*, pp. 2261–2269, 2017.

Josephs, D., Drake, C., Heroy, A. M., and Santerre, J. semg gesture recognition with a simple model of attention. *Machine Learning for Health*, pp. 126–138, 2020.

Kipf, T. N. and Welling, M. Semi-supervised classification with graph convolutional networks. In *Proceedings of the 5th International Conference on Learning Representations*, 2017.

Li, L., Jamieson, K., Rostamizadeh, A., Gonina, E., Hardt, M., Recht, B., and Talwalkar, A. A system for massively parallel hyperparameter tuning. 2020.

Li, L., Khodak, M., Balcan, M.-F., and Talwalkar, A. Geometry-aware gradient algorithms for neural architecture search. In *Proceedings of the 9th International Conference on Learning Representations*, 2021a.

Li, Z., Kovachki, N. B., Azizzadenesheli, K., Liu, B., Bhattacharya, K., Stuart, A., and Anandkumar, A. Fourier neural operator for parametric partial differential equations. In *Proceedings of the 9th International Conference on Learning Representations*, 2021b.

Liu, C., Zoph, B., Neumann, M., Shlens, J., Hua, W., Li, L.-J., Fei-Fei, L., Yuille, A., Huang, J., and Murphy, K. Progressive neural architecture search. In *Proceedings of the European Conference on Computer Vision*, 2018a.

Liu, C., Chen, L.-C., Schroff, F., Adam, H., Hua, W., Yuille, A. L., and Fei-Fei, L. Auto-DeepLab: Hierarchical neural architecture search for semantic image segmentation. In *Proceedings of the IEEE Conference on Computer Vision and Pattern Recognition*, 2019a.

Liu, H., Simonyan, K., Vinyals, O., Fernando, C., and Kavukcuoglu, K. Hierarchical representations for efficient architecture search. 2018b.

Liu, H., Simonyan, K., and Yang, Y. DARTS: Differentiable architecture search. In *Proceedings of the 7th International Conference on Learning Representations*, 2019b.

Liu, Z., Mao, H., Wu, C.-Y., Feichtenhofer, C., Darrell, T., and Xie, S. A convnet for the 2020s. 2022.

Mehrotra, A., Ramos, A. G. C. P., Bhattacharya, S., Dudziak, L., Vipperla, R., Chau, T. C. P., Abdelfattah, M. S., Ishitaq, S. S., and Lane, N. D. Nas-bench-asr: Reproducible neural architecture search for speech recognition. In *International Conference on Learning Representations*, 2021.

Peng, C., Zhang, X., Yu, G., Luo, G., and Sun, J. Large kernel matters — improve semantic segmentation by global convolutional network. *2017 IEEE Conference on Computer Vision and Pattern Recognition (CVPR)*, pp. 1743–1751, 2017.

Pham, H., Guan, M. Y., Zoph, B., Le, Q. V., and Dean, J. Efficient neural architecture search via parameter sharing. In *Proceedings of the 35th International Conference on Machine Learning*, 2018.

Real, E., Aggarwal, A., Huang, Y., and Le, Q. V. Regularized evolution for image classifier architecture search. In *Proceedings of the 33rd AAAI Conference on Artificial Intelligence*, 2019.

Real, E., Liang, C., So, D. R., and Le, Q. V. AutoML-Zero: Evolving machine learning algorithms from scratch. In *Proceedings of the 37th International Conference on Machine Learning*, 2020.

Roberts, N., Khodak, M., Dao, T., Li, L., Ré, C., and Talwalkar, A. Rethinking neural operations for diverse tasks. In *Advances in Neural Information Processing Systems*, 2021.

So, D. R., Liang, C., and Le, Q. V. The evolved transformer. In *International Conference on Machine Learning*, 2019.

Suganuma, M., Ozay, M., and Okatani, T. Exploiting the potential of standard convolutional autoencoders for image restoration by evolutionary search. In *International Conference on Machine Learning*, 2018.

Tu, R., Khodak, M., Roberts, N., and Talwalkar, A. NAS-Bench-360: Benchmarking diverse tasks for neural architecture search. *arXiv*, 2021.

van den Oord, A., Dieleman, S., Zen, H., Simonyan, K., Vinyals, O., Graves, A., Kalchbrenner, N., Senior, A., and Kavukcuoglu, K. Wavenet: A generative model for raw audio. In *Arxiv*, 2016.

Wang, X., Xue, C., Yan, J., Yang, X., Hu, Y., and Sun, K. Mergenas: Merge operations into one for differentiable architecture search. In *IJCAI*, 2020.

Wei, T., Wang, C., Rui, Y., and Chen, C. W. Network morphism. In *International Conference on Machine Learning*, 2016.

Wu, T., Tang, S., Zhang, R., Cao, J., and Li, J. Tree-structured kronecker convolutional network for semantic segmentation. 2019 *IEEE International Conference on Multimedia and Expo (ICME)*, pp. 940–945, 2019.

Xie, S., Zheng, H., Liu, C., and Lin, L. SNAS: Stochastic neural architecture search. In *Proceedings of the 7th International Conference on Learning Representations*, 2019.

Xu, Y., Xie, L., Zhang, X., Chen, X., Qi, G.-J., Tian, Q., and Xiong, H. PC-DARTS: Partial channel connections for memory-efficient architecture search. In *Proceedings of the 8th International Conference on Learning Representations*, 2020.

Yang, Z., Hu, Z., Salakhutdinov, R., and Berg-Kirkpatrick, T. Improved variational autoencoders for text modeling using dilated convolutions. In *International Conference on Learning Representations*, 2017.

Yu, F. and Koltun, V. Multi-scale context aggregation by dilated convolutions. 2016.

Zagoruyko, S. and Komodakis, N. Wide residual networks. In *Proceedings of the British Machine Vision Conference*, 2016.

Zela, A., Elsken, T., Saikia, T., Marrakchi, Y., Brox, T., and Hutter, F. Understanding and robustifying differentiable architecture search. In *Proceedings of the 8th International Conference on Learning Representations*, 2020.

Zhang, K. and Bloom, J. S. deepcr: Cosmic ray rejection with deep learning. *The Astrophysical Journal*, 889(1):24, 2020.

Zhang, Z., Park, C. Y., Theesfeld, C. L., and Troyanskaya, O. G. An automated framework for efficiently designing deep convolutional neural networks in genomics. *Nature Machine Intelligence*, 3(5):392–400, 2021.

Zhou, J. and Troyanskaya, O. G. Predicting effects of noncoding variants with deep learning-based sequence model. *Nature Methods*, 12:931–934, 2015.

Zoph, B., Vasudevan, V., Shlens, J., and Le, Q. V. Learning transferable architectures for scalable image recognition. In *Proceedings of the IEEE Conference on Computer Vision and Pattern Recognition*, 2018.

A. Term Clarification

Since we compare with a variety of methods in the paper, here we clarify some of the terms we use.

what we say	what we are referring to
Best-Automated (Fig. 1a)	WRN, WRN-ASHA, DARTS, DenseNAS, Auto-DL, AMBER
Hand-Designed (Fig. 1a)	Expert architectures in Table 4
AutoML	WRN-ASHA, DARTS, DenseNAS, Auto-DL, AMBER
NAS	DARTS, DenseNAS, Auto-DL, AMBER
WRN	WRN without hyperparameter tuning

B. Asymptotic Analysis

In this section we outline the runtime analysis used to populate the asymptotic complexities in Table 1. All three methods in the table—*mixed-results*, *mixed-weights*, and DASH—are computing the following weighted sum of convolutions:

$$\mathbf{AggConv}_{K,D}(\mathbf{x}) := \sum_{k \in K} \sum_{d \in D} \alpha_{k,d} \cdot \mathbf{Conv}(\mathbf{w}_{k,d})(\mathbf{x}). \quad (6)$$

We consider 1D inputs \mathbf{x} with length n and c_{in} input channels; the convolutions have c_{out} output channels. We view $\mathbf{Conv}(\mathbf{w}_{k,d})(\mathbf{x})$ as having the naive complexity $c_{in}c_{out}kn$ since the deep learning frameworks use the direct (non-Fourier) algorithm. *mixed-results* computes the sum directly, which involves (1) applying one convolution of each size k and dilation to \mathbf{x} at a cost of $c_{in}c_{out}kn$ MULTs and ADDs each for a total cost of $c_{in}c_{out}\bar{K}n$, (2) scalar-multiplying the outputs at a cost of $c_{out}|K||D|n$ MULTs, and (3) summing the results together at a cost of $c_{out}|K||D|n$ ADDs. *mixed-weights* instead (1) multiplies all kernels by their corresponding weight at a cost of $c_{in}c_{out}\bar{K}$ MULTs, (2) zero-pads the results to the largest effective kernel size \bar{D} and adds them together at a cost of $c_{in}c_{out}|K||D|\bar{D}$ ADDs, and (3) applies the resulting \bar{D} -size convolution to the input at a cost of $c_{in}c_{out}\bar{D}n$ MULTs and ADDs. Finally, DASH also (1) does the first two steps of *mixed-weights* at a cost of $c_{in}c_{out}\bar{K}$ MULTs and $c_{in}c_{out}|K||D|\bar{D}$ ADDs but then (2) pads the resulting \bar{D} -size convolution to size n and applies an FFT at a cost of $\mathcal{O}(c_{in}c_{out}n \log n)$ MULTs and ADDs, (3) applies an FFT to \mathbf{x} at a cost of $\mathcal{O}(c_{in}n \log n)$, (4) element-wise multiplies the transformed filters by the inputs at a cost of $c_{in}c_{out}n$ MULTs, (5) adds up c_{in} results for each of c_{out} output channels at a cost of $c_{in}c_{out}n$ MULTs, and (6) applies an iFFT to the result at a cost of $\mathcal{O}(c_{out}n \log n)$.

C. Experiment Details for Fig. 2 and Fig. 3

For the speed tests, we work with the Sequential MNIST dataset, i.e., the 2D 28×28 images are stretched into 1D with length 784. We zero pad or truncate the input to generate data with different input size n . The backbone is 1D WRN with the same structure as introduced in Section 3. The batch size is 128. We run the workflow on a single NVIDIA V100 GPU. The timing results reported are the \log_{10} (combined forward and backward pass time for one search epoch).

In Fig. 2, we study how the size of our multi-scale convolution search space affects the runtimes of *mixed-results*, *mixed-weights*, and DASH for $n = 1000$ (zero-padded MNIST). We define $K = \{3+2(p-1) | 1 \leq p \leq c\}$, $D = \{2^q-1 | 1 \leq q \leq c\}$ and varies c from 1 to 7. Consequently, the number of operations included in the search space grows from 1 to 49.

In Fig. 3, we study how the input size affects the runtimes of the three methods. We fix $K = \{3, 5, 7, 9, 11\}$, $D = \{1, 3, 7, 15, 31\}$ and vary n from 2^5 to 2^{12} .

D. Information About Tasks in NAS-Bench-360

Table 4: Information about evaluation tasks in NAS-Bench-360 (Tu et al., 2021).

Task name	# Data	Data dim.	Type	Learning objective	Expert arch.
CIFAR-100	60K	2D	Point	Classify natural images into 100 classes	DenseNet-BC (Huang et al., 2017)
Spherical	60K	2D	Point	Classify spherically projected images into 100 classes	S2CN (Cohen et al., 2018)
NinaPro	3956	2D	Point	Classify sEMG signals into 18 classes corresponding to hand gestures	Attention Model (Josephs et al., 2020)
FSD50K	51K	2D	Point (multi-label)	Classify sound events in log-mel spectrograms with 200 labels	VGG (Fonseca et al., 2021)
Darcy Flow	1100	2D	Dense	Predict the final state of a fluid from its initial conditions	FNO (Li et al., 2021b)
PSICOV	3606	2D	Dense	Predict pairwise distances between residuals from 2D protein sequence features	DEEPCON (Adhikari, 2019)
Cosmic	5250	2D	Dense	Predict probabilistic maps to identify cosmic rays in telescope images	deepCR-mask (Zhang & Bloom, 2020)
ECG	330K	1D	Point	Detect atrial cardiac disease from a ECG recording (4 classes)	ResNet-1D (Hong et al., 2020)
Satellite	1M	1D	Point	Classify satellite image pixels' time series into 24 land cover types	ROCKET (Dempster et al., 2020)
DeepSEA	250K	1D	Point (multi-label)	Predict chromatin states and binding states of RNA sequences (36 classes)	DeepSEA (Zhou & Troyanskaya, 2015)

E. Evaluation of DASH on NAS-Bench-360

E.1. Backbone Network Structure

E.1.1. 2D TASKS

We use the Wide ResNet 16-4 (Zagoruyko & Komodakis, 2016) as the backbone for all 2D tasks. The original model is made up of 16 3×3 conv followed by 3 WRN blocks with the following structure ($i \in \{1, 2, 3\}$ indicates the block index):

BatchNorm, ReLU	
Conv 1	$16 \times 4 \times i$ ($k = 3, d = 1$) filters, ReLU
Dropout	dropout rate p
BatchNorm, ReLU	
Conv 2	$16 \times 4 \times i$ ($k = 3, d = 1$) filters, stride = $i // 2 + 1$, ReLU
Add residual (apply point-wise conv first if $c_{in} \neq c_{out}$)	

The output block consists of a BatchNorm layer, a ReLU activation, a linear layer, and a final activation layer which we modify according to the task learning objective, e.g., log softmax for classification and sigmoid for dense prediction. We set $p = 0$ in search and tune p as a hyperparameter for retraining. We use the WRN code provided here: <https://github.com/meliketoy/wide-resnet.pytorch>.

E.1.2. 1D TASKS

We use the 1D WRN (Fawaz et al., 2020) as the backbone for all 1D tasks. The model is made up of 3 residual blocks with the following structure:

Conv 1	c_{out} ($k = 8, d = 1$) filters
Dropout	dropout rate p
	BatchNorm, ReLU
Conv 2	c_{out} ($k = 5, d = 1$) filters
Dropout	dropout rate p
	BatchNorm, ReLU
Conv 3	c_{out} ($k = 3, d = 1$) filters
Dropout	dropout rate p
	BatchNorm, ReLU

In the original architecture, $c_{out} = 64$. We set c_{out} to $\min(4^{\text{num_classes}}/10+1, 64)$ to account for simpler tasks with fewer class labels. The output block consists of a linear layer and a activation layer which we modify according to the task learning objective, e.g., log softmax for classification and sigmoid for dense prediction. We set $p = 0$ in search and tune p as a hyperparameter for retraining. We use the 1D WRN code provided here: <https://github.com/okrasolar/pytorch-timeseries>.

E.2. DASH Pipeline Hyperparameters

E.2.1. SEARCH

- Epoch: 100
- Optimizer: SGD (momentum=0.9, nesterov=True, weight_decay=5e-4) for both model weights and architecture parameters
- Model weight learning rate: 0.1 for point prediction tasks, 0.01 for dense tasks
- Architecture parameter learning rate: 0.05 for point prediction tasks, 0.005 for dense tasks
- Learning rate scheduling: decay by 0.2 at epoch 60
- Gradient clipping threshold: 1
- Softmax temperature: 1
- Subsampling ratio: 0.2

E.2.2. HYPERPARAMETER TUNING

- Epoch: 80
- Configuration space:
 - Learning rate: {1e-1, 1e-2, 1e-3}
 - Weight decay: {5e-4, 5e-6}
 - Momentum: {0.9, 0.99}
 - Dropout rate: {0, 0.05}

E.2.3. RETRAINING

- Epoch: 200
- Learning rate scheduling: for 2D tasks, decay by 0.2 at epoch 60, 120, 160; for 1D tasks, decay by 0.2 at epoch 30, 60, 90, 120, 160

E.2.4. TASK-SPECIFIC

2D tasks	CIFAR-100	Spherical	Darcy Flow	PSICOV	Cosmic	NinaPro	FSD50K
Batch size	64	64	10	8	4	128	128
Input size	(32, 32)	(60, 60)	(85, 85)	(128, 128)	(128, 128)	(16, 52)	(96, 101)
Kernel sizes (K)	{3, 5, 7, 9}	{3, 5, 7, 9}	{3, 5, 7, 9}	{3, 5, 7, 9}	{3, 5, 7, 9}	{3, 5, 7, 9}	{3, 5, 7, 9}
Dilations (D)	{1, 3, 7, 15}	{1, 3, 7, 15}	{1, 3, 7, 15}	{1, 3, 7, 15}	{1, 3, 7, 15}	{1, 3, 7, 15}	{1, 3, 7, 15}
Loss (l)	Cross Entropy	Cross Entropy	L2	MSE	BCE	Focal	BCE w. Logits

1D tasks	Satellite	ECG	DeepSEA
Batch size	256	1024	256
Input size	46	1000	1000
Kernel sizes (K)	{3, 7, 11, 15, 19}	{3, 7, 11, 15, 19}	{3, 7, 11, 15, 19}
Dilations (D)	{1, 3, 7, 15}	{1, 3, 7, 15}	{1, 3, 7, 15}
Loss (l)	Cross Entropy	Cross Entropy	BCE w. Logits

F. Accuracy Results on NAS-Bench-360 with Error Bars

Table 5: Performance of DASH and the baselines on tasks in NAS-Bench-360. Results of DASH are averaged over three trials using the models learned after the last epoch. Results of the baselines are taken from (Tu et al., 2021).

	CIFAR-100 0-1 error l	Spherical 0-1 error l	Darcy Flow relative ℓ_2 l	PSICOV MAE ₈ l	Cosmic FNR l
WRN	23.35 \pm 0.05	85.77 \pm 0.71	0.073 \pm 0.001	3.84 \pm 0.053	51.76 \pm 2.09
Expert	19.39\pm0.20	67.41 \pm 0.76	0.008 \pm 0.001	3.35 \pm 0.14	25.29 \pm 1.44
WRN-ASHA	23.39 \pm 0.01	75.46 \pm 0.40	0.066 \pm 0.00	3.84 \pm 0.05	37.53 \pm 10.16
DARTS-GAEA	24.02 \pm 1.92	48.23\pm2.87	0.026 \pm 0.001	2.94\pm0.13	31.15 \pm 3.48
DenseNAS	25.98 \pm 0.38	72.99 \pm 0.95	0.10 \pm 0.01	3.84 \pm 0.15	79.52 \pm 2.20
Auto-DL	-	-	0.049 \pm 0.005	6.73 \pm 0.73	99.79 \pm 0.02
BABY DASH	25.56 \pm 1.37	68.94 \pm 1.3	0.016 \pm 0.002	3.94 \pm 0.54	13.18\pm1.88
DASH	24.37 \pm 0.81	75.44 \pm 2.38	0.0079\pm0.002	3.30 \pm 0.16	15.04 \pm 2.35

	NinaPro 0-1 error l	FSD50K mAP h	ECG F1 score h	Satellite 0-1 error l	DeepSEA AUROC h
WRN	6.78 \pm 0.26	0.08 \pm 0.001	0.57 \pm 0.01	15.49 \pm 0.03	0.60 \pm 0.001
TCN	-	-	0.43 \pm 0.005	16.21 \pm 0.05	0.56 \pm 0.001
Expert	8.73 \pm 0.9	0.38 \pm 0.004	0.72\pm0.00	19.8 \pm 0.00	0.70 \pm 0.24
WRN-ASHA	7.34 \pm 0.76	0.09 \pm 0.03	0.57 \pm 0.01	15.84 \pm 0.52	0.59 \pm 0.002
DARTS-GAEA	17.67 \pm 1.39	0.06 \pm 0.02	0.66 \pm 0.01	12.51 \pm 0.24	0.64 \pm 0.02
DenseNAS	10.17 \pm 1.31	0.36 \pm 0.002	0.60 \pm 0.01	13.81 \pm 0.69	0.60 \pm 0.001
AMBER	-	-	0.67 \pm 0.015	12.97 \pm 0.07	0.68 \pm 0.01
BABY DASH	8.28 \pm 0.62	0.38 \pm 0.01	0.63 \pm 0.001	13.29 \pm 0.108	0.63 \pm 0.017
DASH	6.60\pm0.33	0.40\pm0.008	0.68 \pm 0.007	12.28\pm0.5	0.72\pm0.013

h/l a higher / lower value of the metric indicates better performance.

G. Runtime of DASH on NAS-Bench-360

Table 6: Runtime breakdown for DASH on NAS-Bench-360 tasks evaluated on a NVIDIA V100 GPU.

Task	Search	Hyperparameter Tuning	Retraining	Total
CIFAR-100	1.6	0.15	0.77	2.5
Spherical	1.6	0.25	3.16	5.0
Darcy Flow	0.16	1.6	3.5	5.3
PSICOV	0.88	0.64	14	15
Cosmic	1.6	0.055	5.1	6.8
NinaPro	0.028	0.16	0.11	0.30
FSD50K	0.88	0.88	27	29
ECG	0.18	0.28	0.83	1.3
Satellite	1.8	0.4	4.3	6.5
DeepSEA	0.36	1.6	8.3	10